Supporting Information

Flatz et al. 10.1073/pnas.1013084108

SI Materials and Methods

Animals and Immunization Protocols. Female BALB/c mice between the ages of 6 and 10 wk (NCI/DCT, Jackson Laboratories or Charles River) were used for our experiments. They were housed in the animal facility of the Vaccine Research Center, National Institute of Allergy and Infectious Diseases, National Institutes of Health (NIH), Bethesda, MD. All animal experiments were reviewed and approved by the Animal Care and Use Committee, Vaccine Research Center, National Institute of Allergy and Infectious Diseases, NIH and were performed in accordance with all relevant federal NIH guidelines and regulations. All immunizations were administered intramuscularly. The recombinant replication-defective adenovirus (rAd5) vectors are replication-defective E1-, E3-, and E4-deleted human adenovirus serotype 5-derived vaccines generated as described previously (1). The DNA plasmid used has been extensively described and has been used in clinical trials (2). The recombinant lymphocytic choriomeningitis virus (rLCMV) vectors were generated and titrated as described previously (3, 4).

Flow Cytometry and Cell Sorting. Lympholyte-gradient purified lymphocytes were H2-Dd/PA9-PE tetramer stained for 15 min at 4 °C in PBS. All tetramers were produced by the NIH tetramer core facility. All other fluorochrome-coupled antibodies were obtained from Becton-Dickinson and used as directed by the manufacturer: CD3 Alexa700, CD8a PerCP-Cy5.5, CD127-PE-Cy7, CD62L-APC-Cy7, and in the dump channel CD16-PacBlue and CD32-PacBlue. Sorting for microarray analysis was performed using a FACS Aria directly into cold RNALater (Ambion, Inc.) before freezing at −80 °C.

Intracellular Cytokine Staining. Intracellular cytokine staining was performed as described previously (5). Briefly, spleens were harvested from mice 3 wk after the final immunization, and dissociated over nylon gauze. Single-cell suspensions were washed twice in PBS and 2 million cells per well were distributed into 96-well conical-bottomed plates, in RPMI medium supplemented with 10% FCS containing Brefeldin A (10 μg/mL) and PA9 or an irrelevant peptide (0.1 μg/100 μL). Cells were incubated at 37 °C for 5 h before being washed, stained with VIVID dye (Invitrogen), and fluorescently conjugated antibodies against CD3, CD8, and CD4. Cells were then fixed and permeabilized using BD Cytofix/Cytoperm (BD Pharmingen #554722) and intracellularly stained with antibodies against IFN-γ, TNF-α, and IL2. Cells were analyzed using an LSRII flow cytometer (Becton-Dickinson) and resultant data were analyzed using FlowJo software (FlowJo, Inc.) before being processed using Pestle for analysis using Spice (V4.3), as previously described (6).

Measurement of Single-Cell Gene-Expression Profiles. Single cells were sorted by FACS into 96-well plates containing Platinum Taq polymerase and SuperScript III reverse transcriptase (Invitrogen), a mixture of Taqman primer-probes at 0.2× concentration specific for the transcripts of interest, as listed in Table S2 (Applied Biosystems), CellsDirect One-Shot qRT-PCR buffer (Invitrogen), and SuperaseIn RNase inhibitor. Immediately following cell sorting, samples were centrifuged, incubated at 55 °C for 10 min, and subjected to 18 cycles of PCR (50 °C 15 min then 95 °C for 15 s for the reverse transcription, followed by 18 cycles of 95 °C 15 s and 60 °C 4 min for amplification). Because single cells were sorted directly into a cell lysis reagent in the presence of an RNase inhibitor, any mRNA degradation would have occurred uniformly across all transcripts assessed. This assumption is common to all analyses of relative mRNA expression, including conventional qPCR and microarray cDNA hybridization analysis. Subsequent preamplified single-cell cDNA was stored at −80 °C until analysis. Each cDNA sample was then separated into 96 separate reactions for further qPCR using the BioMark 96.96 dynamic array nanofluidic chip (Fluidigm, Inc.). Briefly, following hydraulic chip priming, 96 preamplified cDNA samples were mixed with a mild detergent loading solution to allow capillary flow, and the samples were added to a 96.96 nanofluidic chip (Fluidigm, Inc.) along with 91 individual Taqman primer-probe mixtures (Applied Biosystems) specific for individual transcripts of interest, as listed in Table S2, allowing a combination of each sample to mix with each probe in every possible combination (a total of 9,216 reactions). The chip was then thermocycled through 40 cycles and fluorescence in the FAM channel was detected using a CCD camera placed above the chip, normalized by ROX (6-carboxy-X-rhodamine) intensity. Data validation and statistical analyses were performed as described below.

Single-Cell Gene-Expression Data Analysis. Amplification signals were analyzed using custom software (Fluidigm, Inc.) and relative mRNA abundance values were calculated using inverse *ct* values normalized to the number of cells sorted. Data were then deconvoluted using scripts written in Python (Python Software Foundation) and Stata (StataCorp, Inc.) Samples where no *Cd8a* signal was detected were removed from the analysis, as well as data for gene assays where no positive signals were observed in any sample, and all samples from plates with any false-positive signals in any null-sorted control wells.

Correlation between microarray data and single-cell data were tested by comparing the proportion of positive cells for each gene between central and effector memory populations and relative fold-change in gene expression, as determined by microarray. Correlation coefficients were calculated using the Spearman's nonparametric test for correlation. A two-stage analysis method was used to identify genes predicting each immunization group. First, univariate preselection analysis was performed using Fisher's exact test to identify a subset of discriminative genes between the three vaccination groups. Second, genes with strong marginal effects after controlling for multiple testing using the Bonferroni threshold were considered for interaction, using the recursive partitioning and regression tree (RPART) method (http://www.mayo.edu/hsr/techrpt/61.pdf). Misclassification error rate was estimated by cross validation for the linear discriminant analysis and the regression-tree classifiers. Regression-tree growth was controlled using the minimum splitting (minsplit) criterion implemented in RPART. This parameter controls the minimum number of observations that must exist in a node for a split to be attempted. RPART models were generated using three different values of minsplit (15, 20, and 25). Fisher's test was done using R's *stats* package. Fisher's linear discriminant analysis is implemented in R's MASS package. Decision tree analysis was carried out using R's *rpart* package. Statistical significance for Fisher's exact test was set after controlling for multiple testing using the Bonferroni method.

Microarray cDNA Hybridization Analysis. Quantification was performed using a spectrophotometer (NanoDrop Technologies) and RNA quality was assessed using the Experion automated electrophoresis system (Bio-Rad Laboratories). Total RNA was

then amplified and labeled using the Illumina TotalPrep RNA Amplification kit, which is based on the Eberwine amplification protocol. This protocol involves a first cDNA synthesis step followed by in vitro transcription for cRNA synthesis. The biotinylated cRNA was hybridized onto Illumina Mouse Chips at 58 °C for 20 h and quantified using an Illumina BeadStation 500GX scanner and Illumina BeadStudio v3 software.

Illumina probe data were exported from BeadStudio as raw data and screened for quality. Samples failing chip visual inspection and control examination were removed. Gene expression data were analyzed using Bioconductor, an open-source software library for the analysis of genomic based on R, which is a language and environment for statistical computing and graphics (www.r-project.org). The R software package was used to first filter out probes with intensities below background in all samples, and then to minimum replace (a surrogate replacement policy) values below background using the mean background value of the built-in Illumina probe controls as an alternative to background subtraction (which may introduce negative values) to reduce "overinflated" expression ratios determined in subsequent steps, and finally quantile normalize the probe intensities. The resulting matrix showing probes as rows and samples as columns was $\log_2$ transformed and used as input for linear modeling using BioConductor linear models for microarray analysis (LIMMA) (7). The Bioconductor LIMMA package was used to identify differentially expressed genes ($P < 0.05$).

1. Wang L, et al. (2009) Delivery of human immunodeficiency virus vaccine vectors to the intestine induces enhanced mucosal cellular immunity. *J Virol* 83:7166–7175.
2. Catanzaro AT, et al. (2007) Phase I clinical evaluation of a six-plasmid multiclade HIV-1 DNA candidate vaccine. *Vaccine* 25:4085–4092.
3. Flatz L, Bergthaler A, de la Torre JC, Pinschewer DD (2006) Recovery of an arenavirus entirely from RNA polymerase I/II-driven cDNA. *Proc Natl Acad Sci USA* 103:4663–4668.
4. Flatz L, et al. (2010) Development of replication-defective lymphocytic choriomeningitis virus vectors for the induction of potent CD8(+) T cell immunity. *Nat Med* 16:339–345.
5. Honda M, et al. (2009) Different vaccine vectors delivering the same antigen elicit CD8+ T cell responses with distinct clonotype and epitope specificity. *J Immunol* 183:2425–2434.
6. Seder RA, Darrah PA, Roederer M (2008) T-cell quality in memory and protection: Implications for vaccine design. *Nat Rev Immunol* 8:247–258.
7. Smyth GK (2005) limma: Linear Models for Microarray Data. Bioinformatics and Computational Biology Solutions Using R and Bioconductor, eds Gentleman R, Carey V, Dudoit S, Irizarry R, Huber W (Springer, New York), pp 397–420.

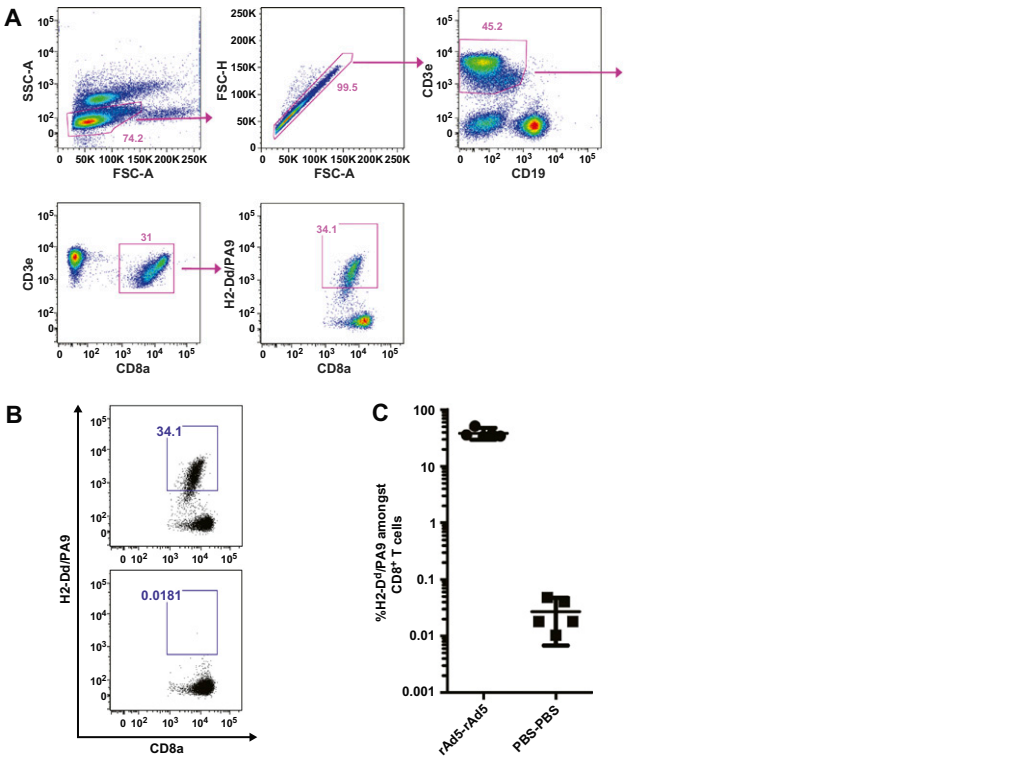

Fig. S1. Confirmation of specificity of tetramer binding. The frequency of H2-Dd/PA9 tetramer binding cells was compared in rAd5-rAd5 immunized animals and unimmunized animals. (*A*) Gating strategy for the identification of antigen-specific cells. (*B*) Representative tetramer binding from rAd5-rAd5 immunized animals vs. unimmunized animals. (*C*) Evaluation of the frequency of tetramer binding in immunized and unimmunized animals expressed as a percentage of total CD3$^+$ CD8$^+$ T cells.

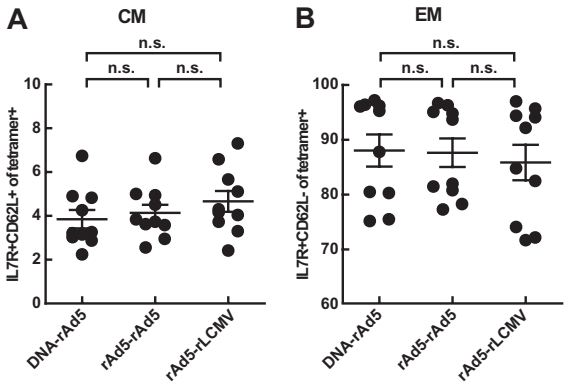

Fig. S2. The proportion of H2-Dd/PA9 tetramer-binding cells with surface protein expression characteristic of central and effector memory phenotypes ($CD62L^+$ $IL7R^+$ and $CD62L^-$ $IL7R^+$, respectively) in mice immunized with the three vaccines was evaluated by flow cytometry. (*A*) The proportion of central memory cells comprising the total antigen-specific response. (*B*) The proportion of effector memory cells comprising the total antigen-specific response.

Other Supporting Information Files

Table S1 (RTF)
Table S2 (DOC)
Table S3 (DOC)
Table S4 (DOC)